Published in final edited form as:
J Nutr. 2008 April ; 138(4): 659–666.

Caco-2 intestinal epithelial cells absorb soybean ferritin by μ_2 subunit (AP2)-dependent endocytosis

Carol D. San Martin[1], **Carolina Garri**[1], **Fernando Pizarro**[3], **Tomas Walter**[3], **Elizabeth C. Theil**[2], and **Marco T. Núñez**[1,*]

[1] Department of Biology, Faculty of Sciences, and Cell Dynamics and Biotechnology Institute, Universidad de Chile, Santiago, Chile

[2] Council for BioIron at CHORI, Children's Hospital Oakland Research Institute, Oakland, CA 94609 and Department of Nutritional Sciences and Toxicology, University of California, Berkeley, CA, 94720

[3] Nutrition and Food Technology Institute, Universidad de Chile, Santiago, Chile

Abstract

Iron deficiency anemia affects ~3 billion people in the 21st century, despite >500 years of medical treatment. Studies show that soybean ferritin, the protein nanocage encasing mineralized iron is a source of nutritional iron but the cellular mechanisms of absorption are unknown. The absorption of iron from soybeans with ferritin in the presence of the endogenous soybean iron chelator phytate, suggests that the mechanism could be different than for reduced ferric or ferrous ions. Here, we investigate a cellular mechanism of iron absorption using recombinant soybean ferritin (SBFn&) and Caco-2 cells grown in bicameral inserts as a model for intestinal cells. Binding, internalization and degradation of exogenous, iron-mineralized SBFn, studied with confocal microscopy and binding of ^{131}I-labeled, iron-mineralized ferritin revealed that: 1- SBFn binds on the apical surface. 2- Binding is saturable, K_d = 7.71 ± 0.88 nmol/L. 3- Internalization of SBFn depended on temperature, concentration and time. 4- Iron inside SBFn rapidly entered the labile iron pool (calcein quenching), and 5- SbFn protein was degraded during the same period that iron entered to the cytosol. SBFn crossed the apical membrane by endocytosis dependent on assembly peptide 2 (AP2) based on sensitivity of ^{131}I-SBFn uptake to hyperosmolarity, acidity and siRNA targeted to the μ2 subunit of AP2, as well as resistance to filipin, a caveolar endocytosis inhibitor. The results support a model of iron absorption from gut ferritin distinct from ion transport and dependent on apical endocytosis followed by mineral dissolution/protein degradation and iron delivery to the cytosolic pool that can function, in part at least to absorb/resorb iron from dietary ferritin/sloughed enterocytes.

Keywords

iron; intestinal absorption; soybean ferritin; endocytosis; AP2

&Abbreviations used: AP2, assembly peptide 2; DF, desferal; DMEM, Dulbecco's Modified Eagle medium; DMT1, divalent metal transporter 1; EDTA, ethylenediaminetetraacetic acid; FAS, ferrous ammonium sulfate; HCP1, heme carrier protein 1; HSFn, horse spleen ferritin; IREG1, Iron Responsive Element GI; LIP, labile iron pool; SBFn, recombinant soybean ferritin; shRNA, short hairpin RNA; siRNA, small interfering RNA; TCA, trichloroacetic acid.

*Address correspondence to: Dr. Marco T. Núñez, Department of Biology, Faculty of Sciences, Universidad de Chile, Las Palmeras 3425, Santiago, Chile. Phone: 562-6787360; Fax: 562-2712983; mnunez@uchile.cl.

Introduction

Cells transport nutrient iron from foods by mechanisms related to the type of iron complex, such as endocytosis for Fe-transferrin from blood and, in the gut, membrane transporters such as heme carrier protein 1 (HCP1) for heme (myoglobin) (1) and divalent metal transporter 1 (DMT1) for ferrous and other divalent cations (2-5). Current data indicate that after internalization, iron from heme or inorganic sources enters the cytosolic labile iron pool (LIP) (reviewed in (6)) and is either delivered to endogenous ferritin for concentration and storage and alter use in iron-protein synthesis, or moved to the basolateral membrane for efflux. Enterocyte iron efflux depends on the iron-export transporter ferroportin or IREG1 (Iron Responsive Element GI) (7-9), in combination with the ferrous oxidase, hephaestin (10). Ferroportin/serum hepcidin interactions regulate efflux rates (De Domenico I, Ward DM, Langelier C, Vaughn MB, Nemeth E, Sundquist WI, Ganz T, Musci G, Kaplan J. The molecular mechanism of hepcidin-mediated ferroportin down-regulation. Mol Biol Cell. 2007 18:2569-78.

Recent studies show that ferritin iron, a biomineral inside a large stable protein nanocage, can be absorbed from foods such as legumes, a particularly rich source [reviewed in (11,12)]. The cellular mechanism used to absorb dietary ferritin iron is unknown. Since ferritin is a very stable protein (13,14) and ferritin iron can be absorbed from soybean ferritin, even in the presence of iron-binding inhibitors such as phytate (15), it is possible at least part of the ferritin iron is absorbed by a mechanism distinct from transport lower molecular weight iron complexes. High-affinity mammalian ferritin binding sites have been reported in reticulocytes, lipocytes, hepatocytes, placenta, brain and kidney (16-19), although the mechanism of ferritin endocytosis has not been elucidated. We investigated soybean ferritin uptake in a model for gut epithelial cells, polarized Caco-2 cells. We observed saturable binding of ferritin at the apical surface (fluorescence microscopy, calcein quenching, and ^{131}I- ferritin uptake/degradation), entry by by AP2-mediated endocytosis (sensitivity to hyperosmolarity, acidity or siRNA for the μ2 subunit of AP2) and degradation of soybean ferritin protein with appearance of the iron in the cytosolic pool. The results show a distinct, a pathway possible for uptake of part of the non-heme dietary iron in ferritin and reabsorption of iron from ferritin in sloughed enterocytes.

Material and Methods

Reagents

Inorganic salts were purchased from Merck. Cell culture media and reagents were from Invitrogen-GIBCO Life Technologies. Buffers and other biochemical reagents were from Sigma Chem. Co.

Ferritin protein

The SBFn coding sequence was subcloned into a pET9a protein expression vector (Novagen) as described (20), and verified by DNA sequencing. As previously described, transfected host *E. coli* Bl21DE3 cells, cultured in LB broth containing betaine and sorbitol (20), were induced with isothiopropylgalactoside and the cells collected and sonicated. Ferritin was isolated from the clarified supernatant fractions as described (21) using chromatography on DEAE-Sephadex and Sephacryl S300. Yields of pure (>95%) protein were ~30 mg/ml. Protein solutions were stored at 4°C in 0.2 mol/L MOPS, 0.2 mol/L NaCl, pH 7.0 or frozen at −20°C in 20% glycerol. A Western blot with soybean ferritin antiserum (22) was used to confirm the identity of the recombinant protein.

^{131}I-labeling of SBFn

SBFn was labeled with ^{131}I (5 mCi/mg protein) using the Iodogen reagent (Pierce Chem. Co.). After iodination, ^{131}I-labeled SBFn was separated from free ^{131}I by 50% ammonium sulfate precipitation followed by extensive dialysis against saline containing the anionic resin AG1 ×8 (BioRad) to trap unincorporated ^{131}I. ^{131}I-labeled SBFn was stored at 4°C and used within 10 days after labeling.

^{131}I-SBFn binding to Caco-2 cells

Human Caco-2 cells (ATCC HTB37) grown on plastic wells for 12-14 days in DMEM supplemented with 10% fetal bovine serum were incubated in serum-free DMEM with concentrations of exogenous, ^{131}I-labeled SBFn that varied between 1 and 16 nmol/L, with or without the addition of 100-fold excess unlabeled ferritin. Binding was performed for 2 h at 4°C. Cells were washed 5 times with ice-cold PBS and detached from the plates with 200 μl 40 mmol/L Tris-HCl pH 7.4, 100 mmol/L NaCl, 1 mmol/L EDTA for 10 min; cells were then collected by centrifugation at 2,000 rpm for 5 min (Hettich Mikro 22R centrifuge, Tuttlingen, Germany). Cell-associated ^{131}I radioactivity was determined in a Cobra II Gamma Radioactivity Counting System (Packard, Meriden, CT). An aliquot of the cell suspension was used for protein determination with bicinchoninic acid (23). Each data point was determined in triplicate. Specific binding was calculated by subtracting binding of ^{131}I-labeled SBFn in the presence of excess unlabeled SBFn (nonspecific binding) from binding without excess unlabeled SBFn. Data were analyzed using GraphPad Prism software (GraphPad Software Inc.). The experimental data were best fit with the Boltzmann sigmoid equation.

^{131}I-SBFn internalization and degradation

Internalization of ^{131}I-SBFn protein was determined by incubating Caco-2 cells in DMEM with 5 nmol/L ^{131}I-SBFn for 0, 15, 30, 60, 90 and 120 min at 37°C. The cells were washed five times with ice-cold PBS, detached from the plastic with 200 μl 40 mmol/L Tris-HCl pH 7.4, 100 mmol/L NaCl, 1 mmol/L EDTA, and collected by centrifugation. The cells were resuspended in 200 μL PBS and incubated overnight at 4°C with 1×10^{-7} mol/L unlabeled SBFn. Cells were then centrifuged and the supernatant and pellet fractions were analyzed for ^{131}I radioactivity as described above. Radioactivity in the supernatant represented surface-bound SBFn, and radioactivity in the cell pellet represented internalized SBFn. To measure ^{131}I-SBFn degradation products released from the cells, the medium, after the cells were removed, was fractionated with 10% TCA (30 min, 4°C); 10μL of FBS was added as a carrier protein and the mixture was separated into insoluble (intact protein) and soluble (small peptides, amino acids) by centrifugation at 10,000 rpm for 5 min (Mikro 22R centrifuge). Radioactivity in the supernatant and precipitated fractions of the culture medium, represented degraded and intact ^{131}I-SBFn, respectively (24-26).

Inhibition of SBFn endocytosis

Caco-2 cells grown in Transwell inserts were incubated for 60 min at 37°C with 5 nmol/L ^{131}I-SBFn in the following media: DMEM (control); DMEM plus 5 μg/ml Filipin III (Sigma Chem. Co.); DMEM plus 0.45 mol/L sucrose (hypertonic), and DMEM with 10 mmol/L acetic acid, which takes advantage of the rapid transport of undissociated acetic acid into the cells with little effect on the pH of the medium; dissociation of acetic acid inside the cells lowers the cytosolic pH. (Sandvig K, Olsnes S, Petersen OW, van Deurs B. Acidification of the cytosol inhibits endocytosis from coated pits.J Cell Biol. 1987 Aug; 105(2):679-89. The cells were washed, and surface-bound ferritin was displaced by an overnight incubation at 4°C with 5×10^{-7} mol/L SBFn. [DELETE: The remaining cell-associated ^{131}I radioactivity represented mostly intact, internalized SBFn.]

Confocal microscopy

Fluorescent reporter linked to secondary antibody—SBFn (5 nmol/L) was added to polarized Caco-2 cells grown on glass cover slips followed by incubation for 60 min. Cells were then fixed and permeabilized, blocked, and incubated overnight with anti-soybean ferritin rabbit antiserum (22) (diluted 1:100), washed, incubated 1 h with Alexa 488–labeled anti-rabbit IgG (Invitrogen-Molecular Probes) and viewed with a Zeiss LSM510 Meta confocal microscope (Carl Zeiss AG).

Fluorescent reporter linked to ferritin—SBFn was coupled to Oregon Green 488 using the FluoReporter® Oregon Green® 488 Protein Labeling kit (Invitrogen-Molecular Probes) to yield SBFn-OG488. Polarized Caco-2 cells cultured on cover slips for 12-14 days were incubated for 60 min at 37°C with 5 nmol/L SBFn-OG488 in the absence or presence of 50 nmol/L unlabeled SBFn. After washing, the cells were fixed with 4% paraformaldehyde, mounted in Gel Mount™ (Sigma Chem. Co.) and observed with a Zeiss LSM 510 Meta confocal laser scanning microscope. Oregon Green fluorescence is a reporter for intact SBFn as well as for many of the larger degradation products.

Transfections

Lipofectamine—Polarized Caco-2 cells were transfected with DNA encoding a short hairpin RNA (shRNA) directed against the μ_2 (AP50) subunit of the AP2 endocytic complex (27). The plasmid pSUPER, encoding the μ2 target sequence GTGGATGCCTTTCGGGTCA (27), was the kind gift of Dr. Philippe Benaroch, INSERM U520 Institut Curie, Paris, France. Caco-2 cells at 60% confluency (8×10^5 cells) were treated with 2.5 μg DNA in lipofectamine (Gibco) for 36 h at 37°C as previously described (28); transfection efficiencies were 20-25%. Lipofectamine-transfected cells were used for immunocytochemistry of μ_2.

Electroporation—Caco-2 cells at 60% confluency were nucleofected with pSUPER containing the μ2 target sequence using the Nucleofector device and the Caco-2 transfection kit following the manufacturer's protocol (amaxa GmbH). Nucleofected cells were used for measurement of SBFn internalization and for Western blot analysis 3-4 days after transfection, at which time the efficiency of transfection was estimated to be 65-75%.

Western blot analysis of μ_2

Cell extracts from control and μ_2-electroporated cells were prepared as described (29). For Western blotting, samples containing 100 μg of protein were boiled in Laemmli sample buffer for 5 min and subjected to SDS-PAGE in 10% acrylamide gels. Proteins were transferred to nitrocellulose membrane and blocked for 1 h at 25°C with 5% nonfat dry milk in blocking saline [20 mmol/L Tris, 0.5 mol/L NaCl, 0.05% (w/v) Tween-20]. Membranes were incubated with anti-μ_2 at a 1:200 dilution overnight at 4°C, rinsed with blocking saline and incubated with horseradish peroxidase–conjugated anti-mouse IgG for 1 h at 25°C. A chemiluminescence assay kit was used for detection (SuperSignal, Pierce Chem. Co.). Chemiluminescence was detected with Fuji photographic film.

Determination of iron incorporation with calcein

Caco-2 cells grown in 2-cm tissue culture wells were incubated for 15 min at 37°C in Hanks' Balanced salt solution containing 5 mmol/L glucose and 1 μmol/L calcein as the lipophilic, acetoxymethyl ester Calcein-AM (Invitrogen-Molecular Probes). Calcein-AM is hydrolyzed by intracellular esterases to the membrane-impermeable adduct calcein. The decrease in calcein fluorescence (485 nm excitation, 530 nm emission) after adding SBFn or ferrous ammonium sulfate (FAS) was quantified using a Cytofluor II plate reader (Applied

Biosystems). After stabilization of the baseline, the medium was supplemented with either 10 nmol/L SBFn or 10 μmol/L FAS. Calcein fluorescence was followed for the next 90 min. To eliminate possible interference from adventitious iron, SBFn was treated with 10 mmol/L diethylenetriaminepentaacetic acid and dialyzed against DMEM prior to the experiment. Parallel wells containing cells loaded with calcein but without further additions were used to determine calcein photobleaching during the experiment. Typically, at the end of the experiment, calcein photobleaching was less than 7% of the initial calcein fluorescence.

Results

Soybean ferritin protein binding, internalization and degradation by Caco-2 cells

Apical internalization of exogenous, SBFn was demonstrated by immunofluorescence using an antibody specific for SBFn (Figure 1); soybean ferritin polypeptides >10 kDa are immunoreactive (22). Overlays of fluorescence and phase contrast images from cells, incubated without or with SBFn prior to immunodetection, showed the specificity of anti-SBFn (Figure 1A). There was a gradient of decreasing immunoreactivity as the distance from the apical surface of the cell increased, with most of the reactivity in the apical half of the cells (Figure 1B and 1C).

Specific binding of SBFn to the apical surface of Caco-2 cells

To determine the properties of SBFn interactions with the apical membrane of Caco-2 cells, we analyzed binding of SBFn labeled to the apical membrane Caco-2 cells (Figure 2) with ^{131}I SBFn. Non-specific binding (^{131}I remaining after incubation with 100-fold excess of unlabelled SBFn) was subtracted from overall binding and equaled ~ 15% of the total binding at 10 nM ^{131}I-SBFn. The binding data were adjusted with the hyperbola function of GraphPad 5.0. Scatchard analysis indicated an apparent $K_d = 7.71 \pm 0.88\ 10^{-9}$ mol/L for exogenous soybean ferritin and Caco-2 cells that is in the range of $K_{0.5}$ values, 5.1×10^{-10} mol/L, 4.1×10^{-8} mol/L and 4.65×10^{-9} mol/L for heterologous, mammalian ferritins binding to lipocytes (18), erythroid precursors (30) and mouse brain (19), respectively. These results suggest the presence of specific receptors for SBFn in the apical surface of the cells. Similar results were obtained using HSFn (data not show); hence, the putative receptor recognizes Fn of both plant and animal origin.

Fate of internalized SBFn protein

The kinetics of binding of SBFn by Caco-2 cells was investigated by incubating Caco-2 cells with ^{131}I-labeled SBFn in the apical medium (Figure 3). The rate of binding in the initial phase was 0.73 ± 0.13 fmol per mg of protein, and the steady state at about 30 min of incubation (Figure 3A). After 1 h incubation at 37°C, surface binding was 1.5 ± 0.4 fmol per mg of protein.

The majority of the cell-associated ^{131}I-SBFn was intact protein based on TCA precipitation (87.3 ± 4.4%). Since the TCA-precipitable cell-associated ^{131}I-SBFn was not displaced in an overnight incubation at 4°C with 500 nmol/L unlabeled SBFn, the ^{131}I-SBFn was inside the cells. However, after 1 h at 37°C, 30% of the total ^{131}I-SBFn was TCA-soluble and the degradation products appeared in the medium as TCA-soluble ^{131}I. Actively metabolizing cells were necessary to convert the internalized ^{131}I-SBFn to TCA-soluble ^{131}I in the medium (Fig. 3C), since incubation with or without cells at 4°C, or without cells at 37°C, converted only 5% of the ^{131}I-SBFn to TCA soluble fragments. The increase in ^{131}I in the medium after 1 h of incubation was equivalent to 130.3 ± 15.6 fmol/mg protein, compared to the cells, which had 10.0 ± 1.4 fmol/mg protein of SBFn (Fig. 3B); the amount of ^{131}I released into the medium was > than 100-fold that remaining in the cells. Thus, upon interaction with the cell, SBFn was rapidly internalized and then degraded.

Fate of the iron in internalized soybean ferritin

To determine the potential physiological relevance of soybean ferritin binding and internalization by polarized Caco-2 cells, we examined the entry of ferritin iron into the cytosolic iron pool. For iron, the pool is named the LIP (Labile Iron Pool) because many iron-proteins and cofactors have such high affinities for iron that only iron bound to cytosolic components with affinities lower than the probe can be be measured (31). Calcein fluorescence was used to analyze the LIP (32,33); calcein fluorescence is quenched upon binding either Fe^{+2} or Fe^{+3}. Photobleaching during the experiment was monitored as the fluorescence of cell calcein without added iron and FAS (ferrous ammonium sulfate) was used as a positive control for DMT transport of iron and entry into the LIP (34). When SBF or horse spleen ferritin (HSFn) were used as iron sources, calcein fluorescence decreased more rapidly than in the controls indicating that iron from either plant or animal ferritin entered the cytosolic LIP (Figure 4A). Changes in calcein fluorescence were best fit to a one-phase, exponential decay model. Desferal did not alter the entry of ferritin iron to the LIP, confirming the absence of adventitious iron in the mineralized ferritin samples, and more importantly, emphasizing the separation of iron entering cells in ferritin iron from iron entering via DMT1.

We next explored the effects of inhibitors of endocytosis on the entry of ferritin iron into the LIP for three reasons: 1- Our studies (Fig 2,3) suggested the presence of ferritn receptors also suggested in other cell types (16-19). 2- The desferal resistance of ferritin Fe entry to the LIP contrasting with DMT1-mediated uptake of FAS, indicated a different pathway for iron in the two chemical forms (Fig.4A); 3- the large size of ferritin (12 nm diameter compared to 0.2 nm of hydrated ferrous ions). The inhibitors of endocytosis used were cytoplasmic acidification, which interferes with budding of clathrin-coated vesicles from the plasma membrane and incubation in hypertonic medium, which prevents clathrin and AP2 from interacting (35-37) Both inhibitors of endocytosis tested inhibited entry of ferritin iron into the cytoplasmic pool (Fig. 4B).

The functionality of SBFn binding reported above (Figure 2) was further explored by determination of SBFn iron entrance into the cytosol labile iron pool as a function of SBFn concentration (Figure 4C and 4D). Increased SBFn concentration resulted in increased initial rates of calcein quenching, with a tendency to reach a plateau (Figure 4C). Plotting the initial rate of iron entrance as a function of SBFn concentration resulted in a hyperbolic curve with a $K_{0.5} = 3.29 \pm 0.51$, a value close to the $K_{0.5}$ ^{131}I-SBFn binding constant ($5.77 \pm 1.63\ 10^{-9}$ mol/L), a clear indication that most of the specific binding of. SBFn or HSFn to the cell surface resulted in an effective internalization and degradation of the proteins.

Inhibition of SBFn internalization by acidification and hyperosmolarity and insensitivity of internalization to filipin

To further investigate the pathway(s) of SBFn protein internalization in human intestinal epithelial Caco-2 cells, we examined the sub-cellular distribution of SBFn labeled with Oregon Green (Figure 5A) after incubation for different periods of time. After short incubation periods (5-15 min), an apical-to-basal gradient of the label was observed, confirming that SBFn entered from the apical side of the cells. Intracellular fluorescence increased up to 30 min, when strong intracellular signals both in the apical and the basal cytosolic domain were evident. The signal from Oregon green–labeled SBFn on the basal side of the cell likely indicates degraded SBFn because it was not detected with anti-SBFn, which recognizes native SBFn (Figure 1); this suggests that internalized SBFn is degraded in an apical-to-basal direction.

Effects inhibitors of caveolar [Filipin] or clathrin dependent endocytosis [hyperosmolaric sucrose or at low pH (5.0)] were studied next by preincubating cells with the inhibitors and analyzing the distribution of Oregon Green-labeled SBFn or ^{131}I SBFn. Filipin, a sterol-binding agent that binds cholesterol, a major component of glycolipid microdomains and caveolae (38-40), was used to disrupt caveolar structure and function. When the inhibitors affected clathrin-mediated endocytosis (hypertonicity or low pH), Oregon Green fluorescence was concentrated at the apical limit, whereas in control cells fluorescence was distributed to both the apical and basal domains (Fig. 5B). Filipin, by contrast, had no effect on SBFn internalization except a slight decrease in apical labeling (Fig. 5B). Similarly, ^{131}I-labeled SBFn internalization was strongly inhibited by preincubation of the cells in hypertonic or acidified media, and filipin had no effect (Fig. 5C). The data with inhibitors (Fig. 5) combined with those of the calcein study (Fig. 4) show that both Fe transfer from SBFn to the LIP and SBFn protein internalization possibly use a AP2 mediated pathway.

Inhibition of SBFn internalization by RNA interference of μ_2, a subunit of the AP2 complex

Further evidence for endocytosis of SBFn was sought by inhibiting the expression of the μ_2 subunit of the AP2 endocytic complex with siRNA (Figure 6). Western blot analysis of transfected cells revealed decreased expression of the μ_2 protein (Figure 6A), which correlated with decreased intracellular SBFn, as demonstrated by decreased ^{131}I-labeled SBFn uptake (Figure 6B). Endocytosis of IgG, that undergoes clathrin-mediated endocytosis in intestinal cells (41,42), was also inhibited in μ2 shRNA treated cells (Figure 6B). The sensitivity of ferritin and IgG internalization to μ_2 expression supports the hypothesis that ferritin uptake is facilitated by an AP2-mediated endocytosis pathway.

Discussion

Recent studies show that ferritin iron is absorbed by mammals from plant [reviewed in (12)]. This observation is potentially important for the treatment of iron deficiency anemia, a condition affecting ~3 billion people in the 21st century despite half a millennium of medical diagnoses and treatments. Moreover, the difference in the structure of ferritin iron, a solid mineral of hundreds to thousands of atoms inside a large, hydrophilic protein cage, compared to the single iron atoms in lipid-soluble heme or the single ferrous ion coordinated to six water molecules raises the possibility that ferritin is recognized by different molecules on the surface of intestinal cells, compared to the more extensively studied forms of iron in heme and ferrous salts. All cells synthesize ferritin, the spherical, protein nanocages with iron biominerals inside, at some time during differentiation or maturation (22). In animal cells, in addition to the generic Fer H-type gene found universally in animals, plants and bacteria, a catalytically inactive subunit, FerL, is expressed that coassembles with the FerH subunit in variable amounts (43,44), making endogenous intestinal cell ferritin different from plant ferritin. Each animal ferritin subunit also has a distinctive N-terminal extension (45).

In this study, we showed that soybean ferritin entered cells from the apical surface of Caco-2 cells by a AP2-mediated endocytic pathway. Based on the calcein fluorescence quenching data, once internalized, soybean ferritin iron entered the common intracellular iron pool, indicating its physiological relevance, and the soybean ferritin protein was degraded as demonstrated by the release of ^{131}I into the TCA-soluble fraction of the medium at a rate of 130.3 ± 15.6 fmol per mg of protein. Thus, gut absorption of plant ferritin via ferritin endocytosis could provide iron for bodily needs, and may explain the presence of ferritin-rich legumes among the earliest plants domesticated by humans (46).

Endocytosis of iron as a ferritin mineral is much more efficient than transport of individual iron atoms across the cell membrane as ferrous iron via DMT1, for example, as ferritin can

contain a mineral with thousands of iron atoms (43,44). Soybean ferritin in nature has ~ 800 ferric atoms (45); reconstituted, recombinant SBFn used here had an average of 450 ferric atoms. With only one endocytototic cycle of a soybean ferritin molecule, 450 iron atoms can enter the cell contrasting with only one/ DMT1 transport cycle. However, in the cultured Caco-2 cells, at the observed rate of 130 fmol of internalized ferritin/h/mg cell protein, the contribution of iron to the cytoplasmic pool would be 58 pmol Fe/h/mg cell protein, a value in the middle of the range of values of 30 and 108 pmol Fe/h/mg cell protein for ferrous sulfate??? or heme iron by Caco-2 cells, respectively (47,48).

Ferritin uptake has been observed in liver hepatocytes (49), lipocytes (18), erythroid precursors (30), mouse brain (19) and placental microvilli membrane (16). The finding that immunoglobulin-domain and mucin-domain protein 1 (TIM-1) in kidney and liver is a specific receptor for endogenous H-ferritin in mouse (17) complemented earlier studies of saturable cell surface sites as participants in ferritin uptake. In addition, the suggestion of gut iron resorption from endogenous ferritin released during enterocyte turnover (50) could depend on ferritin/cell surface interactions. Regulation of ferritin uptake by cellular iron status has been observed for some cell types, such as erythroid precursors and cells in the placental microvilli (16,30), but iron regulation is absent in liver hepatocytes (49), possibly because of the specialized role of hepatocytes in storing excess body iron. Ferritin uptake by endocytosis through the apical membrane of Caco-2 cells is an extremely efficient uptake of iron through the cascade of ferritin internalization, mineral dissolution, and iron release.

Current molecular knowledge of cellular iron transport is limited to entry of ferrous ions (DMT1) or heme (HCP1) on the apical surface and the release of ferrous via ferroportin, at the basolateral surface of gut absorptive epithelial cells. How iron moves from one side of the cell to the other, and where, and/or whether, the two pathways converge within the cell, have remained a mystery. Soybean ferritin endocytosis, identified here in intestinal Caco-2 cells, and easily distinguished immunologically from endogenous ferritin, may be a valuable tool for tracking iron across cells, identifying the point(s) of convergence in trafficking of the different iron complexes entering cells by different pathways, and for a more complete understanding of iron nutrition from different sources.

Acknowledgments

The authors are grateful to Brie Fuqua for preparing the protein expression vector and isolation of soybean ferritin and to Victoria Tapia and Lorena Sarragoni for help with confocal microscopy.

The work of the authors has been supported by FONDECYT project 1050068 (CG, FP, CSM, MTN and TW) and by NIH grant DK20251 (ECT).

Literature Cited

1. Shayeghi M, Latunde-Dada GO, Oakhill JS, Takeuchi K, Laftah AH, Halliday N, Khan Y, Warley A, McCann FE, et al. Identification of an intestinal heme transporter. Cell. 2005; 122:789–801. [PubMed: 16143108]
2. Fleming MD, Romano MA, Su MA, Garrick LM, Garrick MD, Andrews NC. Nramp2 is mutated in the anemic Belgrade (b) rat: evidence of a role for Nramp2 in endosomal iron transport. Proc Natl Acad Sci U S A. 1998; 95:1148–1153. [PubMed: 9448300]
3. Fleming MD, Trenor CC 3rd, Su MA, Foernzler D, Beier DR, Dietrich WF, Andrews NC. Microcytic anaemia mice have a mutation in Nramp2, a candidate iron transporter gene. Nat Genet. 1997; 16:383–386. [PubMed: 9241278]
4. Garrick MD, Dolan KG, Horbinski C, Ghio AJ, Higgins D, Porubcin M, Moore EG, Hainsworth LN, Umbreit JN, et al. DMT1: a mammalian transporter for multiple metals. Biometals. 2003; 16:41–54. [PubMed: 12572663]

5. Gunshin H, Mackenzie B, Berger UV, Gunshin Y, Romero MF, Boron WF, Nussberger S, Gollan JL, Hediger MA. Cloning and characterization of a mammalian proton-coupled metal-ion transporter. Nature. 1997; 388:482–488. [PubMed: 9242408]

6. Kruszewski M. Labile iron pool: the main determinant of cellular response to oxidative stress. Mutat Res. 2003; 531:81–92. [PubMed: 14637247]

7. Donovan A, Brownlie A, Zhou Y, Shepard J, Pratt SJ, Moynihan J, Paw BH, Drejer A, Barut B, et al. Positional cloning of zebrafish ferroportin1 identifies a conserved vertebrate iron exporter. Nature. 2000; 403:779–781.

8. McKie AT, Marciani P, Rolfs A, Brennan K, Wehr K, Barrow D, Miret S, Bomford A, Peters TJ, et al. A novel duodenal iron-regulated transporter, IREG1, implicated in the basolateral transfer of iron to the circulation. Mol Cell. 2000; 5:299–309. [PubMed: 10882071]

9. Abboud S, Haile DJ. A novel mammalian iron-regulated protein involved in intracellular iron metabolism. J Biol Chem. 2000; 275:19906–19912. [PubMed: 10747949]

10. Frazer DM, Vulpe C, McKie AT, et al. Cloning and gastrointestinal expression of rat hephaestin: relationship to other iron transport proteins. Am J Physiol Gastrointest Liver Physiol. 2001; 281:G931–939. [PubMed: 11557513]

11. Briat JF, Lobreaux S, Grignon N, Vansuyt G. Regulation of plant ferritin synthesis: how and why. Cell Mol Life Sci. 1999; 56:155–166. [PubMed: 11213255]

12. Theil EC. Iron, ferritin, and nutrition. Annu Rev Nutr. 2004; 24:327–343. [PubMed: 15189124]

13. Listowsky I, Blauer G, Enlard S, Betheil JJ. Denaturation of horse spleen ferritin in aqueous guanidinium chloride solutions. Biochemistry. 1972; 11:2176–2182. [PubMed: 5063666]

14. Santambrogio P, Levi S, Arosio P, Palagi L, Vecchio G, Lawson DM, Yewdall SJ, Artymiuk PJ, Harrison PM, et al. Evidence that a salt bridge in the light chain contributes to the physical stability difference between heavy and light human ferritins. J Biol Chem. 1992; 267:14077–14083. [PubMed: 1629207]

15. Murray-Kolb LE, Welch R, Theil EC, Beard JL. Women with low iron stores absorb iron from soybeans. Am J Clin Nutr. 2003; 77:180–184. [PubMed: 12499339]

16. Liao QK, Kong PA, Gao J, Li FY, Qian ZM. Expression of ferritin receptor in placental microvilli membrane in pregnant women with different iron status at mid-term gestation. Eur J Clin Nutr. 2001; 55:651–656. [PubMed: 11477463]

17. Chen TT, Li L, Chung DH, Allen CD, Torti SV, Torti FM, Cyster JG, Chen CY, Brodsky FM, et al. TIM-2 is expressed on B cells and in liver and kidney and is a receptor for H-ferritin endocytosis. J Exp Med. 2005; 202:955–965. [PubMed: 16203866]

18. Ramm GA, Britton RS, O'Neill R, Bacon BR. Identification and characterization of a receptor for tissue ferritin on activated rat lipocytes. J Clin Invest. 1994; 94:9–15. [PubMed: 8040296]

19. Hulet SW, Powers S, Connor JR. Distribution of transferrin and ferritin binding in normal and multiple sclerotic human brains. J Neurol Sci. 1999; 165:48–55. [PubMed: 10426147]

20. Blackwell JR, Horgan R. A novel strategy for production of a highly expressed recombinant protein in an active form. FEBS Lett. 1991; 295:10–12. [PubMed: 1765138]

21. Jin W, Takagi H, Pancorbo NM, Theil EC. “Opening” the ferritin pore for iron release by mutation of conserved amino acids at interhelix and loop sites. Biochemistry. 2001; 40:7525–7532. [PubMed: 11412106]

22. Ragland M, Theil EC. Ferritin (mRNA, protein) and iron concentrations during soybean nodule development. Plant Mol Biol. 1993; 21:555–560. [PubMed: 8443348]

23. Smith PK, K R, Hermanson GT, Mallia AK, Gartner FH, Provenzano MD, Fujimoto EK, Goeke NM, Olson BJ, Klenk DC. Measurement of protein using bicinchoninic acid. Anal Biochem. 1985; 150:76–85. [PubMed: 3843705]

24. Goldstein JL, Brown MS. Binding and degradation of low density lipoproteins by cultured human fibroblasts. Comparison of cells from a normal subject and from a patient with homozygous familial hypercholesterolemia. J Biol Chem. 1974; 249:5153–5162. [PubMed: 4368448]

25. Bos CR, Shank SL, Snider MD. Role of clathrin-coated vesicles in glycoprotein transport from the cell surface to the Golgi complex. J Biol Chem. 1995; 270:665–671. [PubMed: 7822293]

26. Zhao B, Li Y, Buono C, Waldo SW, Jones NL, Mori M, Kruth HS. Constitutive receptor-independent low density lipoprotein uptake and cholesterol accumulation by macrophages

differentiated from human monocytes with macrophage-colony-stimulating factor (M-CSF). J Biol Chem. 2006; 281:15757–15762. [PubMed: 16606620]

27. Dugast M, Toussaint H, Dousset C, Benaroch P. AP2 clathrin adaptor complex, but not AP1, controls the access of the major histocompatibility complex (MHC) class II to endosomes. J Biol Chem. 2005; 280:19656–19664. [PubMed: 15749704]
28. Arredondo M, Tapia V, Rojas A, Aguirre P, Reyes F, Marzolo MP, Núñez MT. Apical distribution of HFE-beta2-microglobulin is associated with inhibition of apical iron uptake in intestinal epithelia cells. Biometals. 2006; 19:379–388. [PubMed: 16841247]
29. Aguirre P, Mena N, Tapia V, Arredondo M, Nunez MT. Iron homeostasis in neuronal cells: a role for IREG1. BMC Neurosci. 2005; 6:3. [PubMed: 15667655]
30. Gelvan D, Fibach E, Meyron-Holtz EG, Konijn AM. Ferritin uptake by human erythroid precursors is a regulated iron uptake pathway. Blood. 1996; 88:3200–3207. [PubMed: 8874221]
31. Breuer W, Epsztejn S, Cabantchik ZI. Iron acquired from transferrin by K562 cells is delivered into a cytoplasmic pool of chelatable iron(II). J Biol Chem. 1995; 270:24209–24215. [PubMed: 7592626]
32. Epsztejn S, Kakhlon O, Glickstein H, Breuer W, Cabantchik I. Fluorescence analysis of the labile iron pool of mammalian cells. Anal Biochem. 1997; 248:31–40. [PubMed: 9177722]
33. Kakhlon O, Cabantchik ZI. The labile iron pool: characterization, measurement, and participation in cellular processes(1). Free Radic Biol Med. 2002; 33:1037–1046. [PubMed: 12374615]
34. Arredondo M, Munoz P, Mura CV, Nunez MT. DMT1, a physiologically relevant apical Cu1+ transporter of intestinal cells. Am J Physiol Cell Physiol. 2003; 284:C1525–1530. [PubMed: 12734107]
35. Daukas G, Zigmond SH. Inhibition of receptor-mediated but not fluid-phase endocytosis in polymorphonuclear leukocytes. J Cell Biol. 1985; 101:1673–1679. [PubMed: 4055891]
36. Hansen S, Sandvig K, van Deurs B. Clathrin and HA2 adaptors: effects of potassium depletion, hypertonic medium, and cytosol acidification. J Cell Biol. 1993; 121:61–72. [PubMed: 8458873]
37. Sandvig K, Olsnes S, Petersen OW, van Deurs B. Acidification of the cytosol inhibits endocytosis from coated pits. J Cell Biol. 1987; 105:679–689. [PubMed: 2887575]
38. Rothberg KG, Ying YS, Kamen BA, Anderson RG. Cholesterol controls the clustering of the glycophospholipid-anchored membrane receptor for 5-methyltetrahydrofolate. J Cell Biol. 1990; 111:2931–2938. [PubMed: 2148564]
39. Rothberg KG, Heuser JE, Donzell WC, Ying YS, Glenney JR, Anderson RG. Caveolin, a protein component of caveolae membrane coats. Cell. 1992; 68:673–682. [PubMed: 1739974]
40. Orlandi PA, Fishman PH. Filipin-dependent inhibition of cholera toxin: evidence for toxin internalization and activation through caveolae-like domains. J Cell Biol. 1998; 141:905–915. [PubMed: 9585410]
41. Benlounes N, Chedid R, Thuillier F, Desjeux JF, Rousselet F, Heyman M. Intestinal transport and processing of immunoglobulin G in the neonatal and adult rat. Biol Neonate. 1995; 67:254–263. [PubMed: 7647150]
42. Rodewald R, Kraehenbuhl JP. Receptor-mediated transport of IgG. J Cell Biol. 1984; 99:159s–164s. [PubMed: 6235233]
43. Harrison PM, Arosio P. The ferritins: molecular properties, iron storage function and cellular regulation. Biochim Biophys Acta. 1996; 1275:161–203. [PubMed: 8695634]
44. Liu X, Theil EC. Ferritin as an iron concentrator and chelator target. Ann NY Acad Sci. 2005; 1054:136–140. [PubMed: 16339659]
45. Ragland M, Briat JF, Gagnon J, Laulhere JP, Massenet O, Theil EC. Evidence for conservation of ferritin sequences among plants and animals and for a transit peptide in soybean. J Biol Chem. 1990; 265:18339–18344. [PubMed: 2211706]
46. Hancock, JF. Plant Evolution and the Origin of Crop Species. 2nd. CABI Publishing; Cambridge, MA: 2004.
47. Arredondo M, Muñoz P, Mura CV, Núñez MT. HFE inhibits apical iron uptake by intestinal epithelial (Caco-2) cells. Faseb J. 2001; 15:1276–1278. [PubMed: 11344112]

48. Mendiburo MJ, Flores S, Pizarro F, Arredondo M. Heme oxygenase 1 overexpression increases iron fluxes in caco-2 cells. Biol Res. 2006; 39:195–197. [PubMed: 16629181]

49. Adams PC, Chau LA. Hepatic ferritin uptake and hepatic iron. Hepatology. 1990; 11:805–808. [PubMed: 2347554]

50. Hunt JR, Roughead ZK. Nonheme-iron absorption, fecal ferritin excretion, and blood indexes of iron status in women consuming controlled lactoovovegetarian diets for 8 wk. Am J Clin Nutr. 1999; 69:944–952. [PubMed: 10232635]

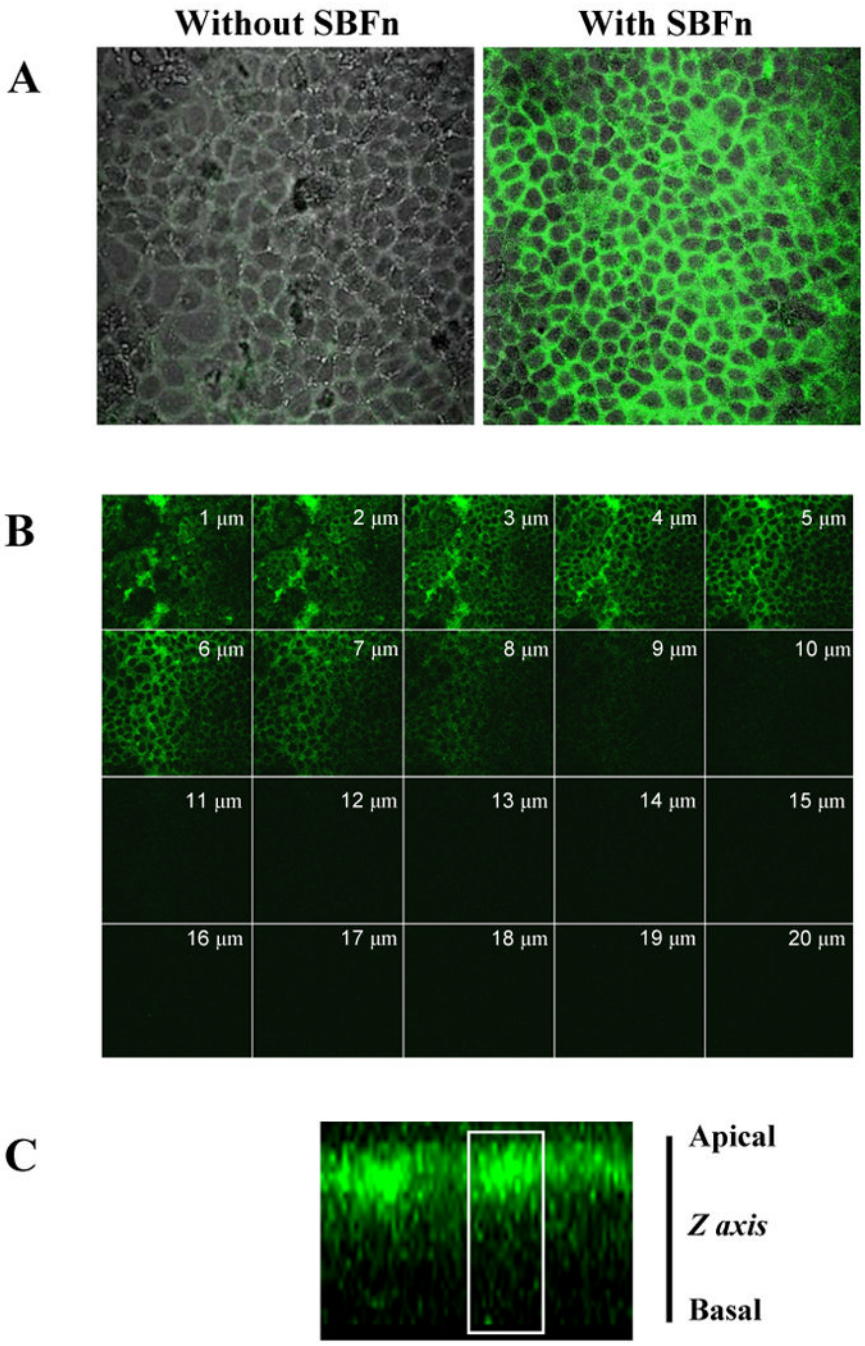

Figure 1. Immunofluorescence detection of SBFn inside cells

Caco-2 cells grown on glass cover slips were incubated for 60 min with 5 nmol/L SBFn. Cells were then fixed and permeabilized, incubated with anti-soybean ferritin rabbit antiserum, detected with Alexa 488–labeled anti-rabbit IgG and viewed under a confocal microscope. A: Overlays of fluorescence and phase contrast images from cells incubated without or with SBFn prior to immunodetection, showing that the antibody did not label endogenous Caco-2 cell ferritin. B: Gallery of 1-µm optical slices from the apical to basal membrane. Staining for SBFn was prominent in the apical domain. C: Z-axis projection of confocal optical slices revealing SBFn immunoreactivity mostly in the upper half of the cell. A cell contour, in white, derived from phase contrast images, is shown as a reference.

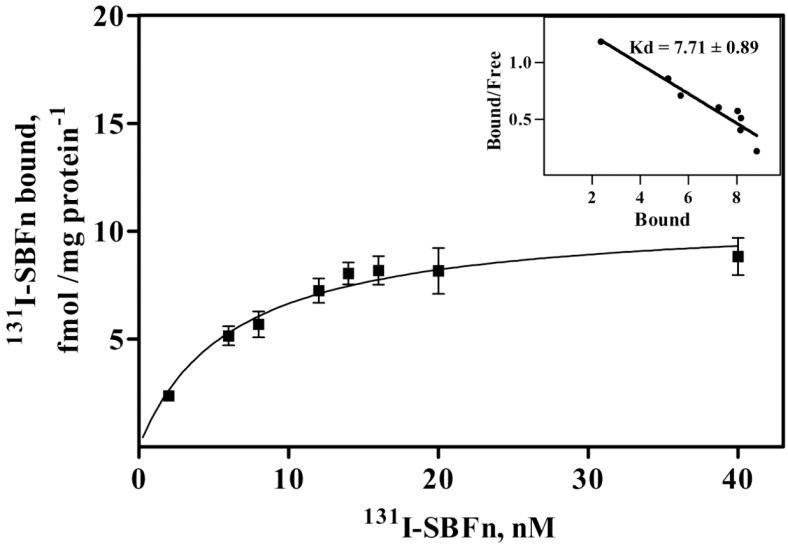

Figure 2. Effect of ^{131}I-labeled SBFn concentration on saturation of Caco-2 cell binding sites

Caco-2 cells grown in bicameral transwells were incubated from the apical chamber for 2 h at 4°C with various concentrations of ^{131}I-labeled SBFn. Shown is the specific ^{131}I-labeled SBFn binding after discounting binding in the presence of a 100-fold excess unlabeled SBFn. Points were adjusted with a hyperbolic function using the GraphPad 5.0 program. The results are presented as the means of four independent experiments, and the error bars indicate the SEM. The insert shows the Scatchard analysis of binding data.

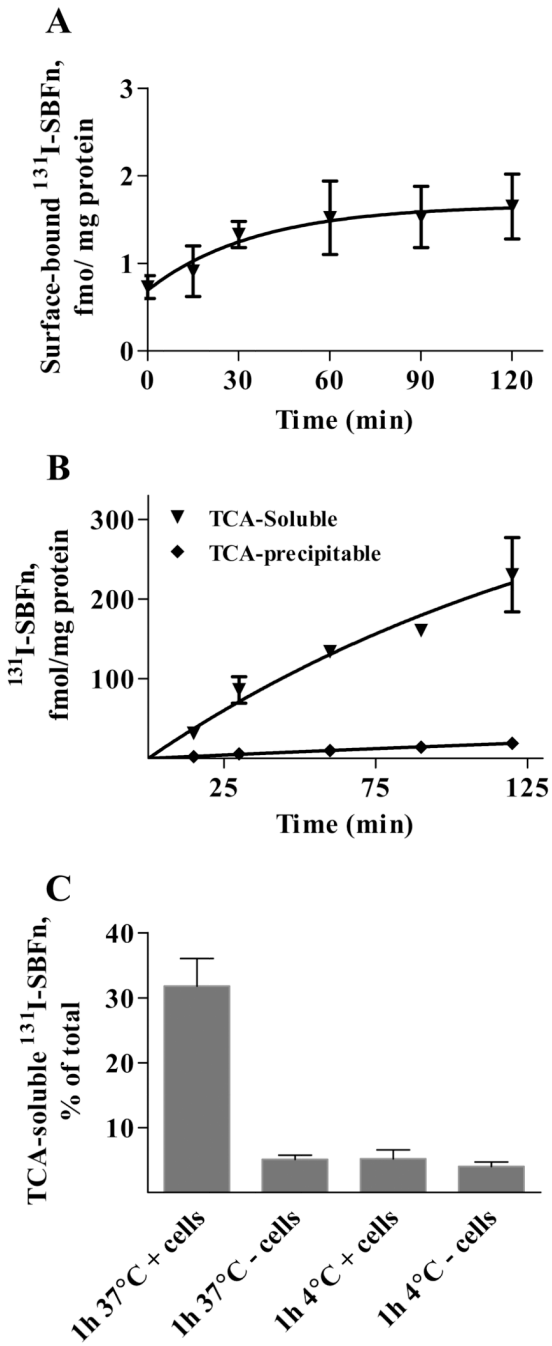

Figure 3. Fate of SBFn in Caco-2 Cells

Polarized Caco-2 cells were incubated with 5 nmol/L ^{131}I-labeled SBFn at 37°C for different times. Protein binding to the cell surface, determined by displacement of surface ^{131}I-labeled SBFn by unlabeled SBFn (A), and protein degradation, determined as the soluble ^{131}I radioactivity following 10% TCA precipitation (B), were measured as described in the Materials and Methods. C: The effects of cells and temperature on the release of ^{131}I-ferritin degradation products were analyzed as described in the Methods section. The results are presented as the means and SD for three independent experiments done in triplicates.

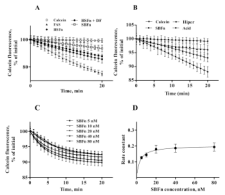

Figure 4. Incorporation of SBFn iron into the LIP

A: entry of exogenous iron into polarized calcein-loaded Caco-2 cells was measured as the quenching of calcein fluorescence. Fluorescence was monitored every 1 min for 20 min. Iron-donating capacity of 10 μmol/L FAS (ferrous ammonium sulfate), 10 nmol/L HSFn (horse spleen ferritin), 10 nmol/L HSFn with 10 μmol/L DF (given simultaneously), and 10 nmol/L SBFn was determined. Calcein photobleaching during the experiment, determined in parallel using cells with calcein but no added iron, was less than 2% of the initial fluorescence after 20 min of incubation. B: Iron-donating capacity of 10 nmol/L SBFn in DMEM (SBFn), DMEM + 10 mmol/L acetic acid, pH 5.0 (Acid) or DMEM + 0.45 mol/L sucrose (Hiper). C: Calcein-loaded Caco-2 cells were incubated for the stated times with SBFn in the 5-80 nM range, and iron incorporation into the labile iron pool was detected by the quenching of intracellular calcein. Curves were adjusted with a single exponential decay function using the GraphPad 5.0 program. D: the rate constants derived form curves in Figure 2B were plotted as a function of SBFn concentration. An apparent KD = 3.29 ± 0.51 nM was obtained. Data points represent Mean ± SEM of triplicates. Shown are representative experiments (N = 3).

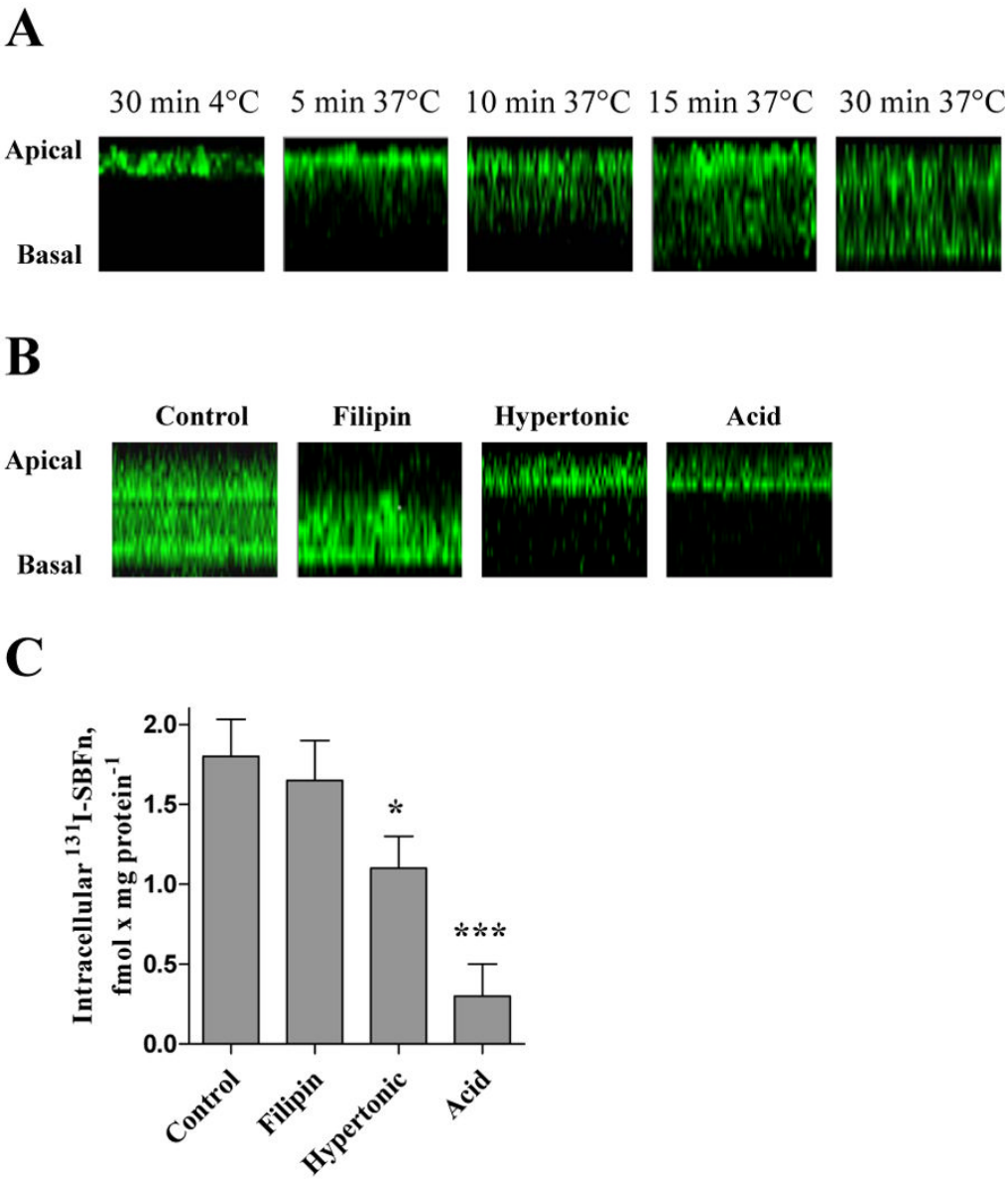

Figure 5. Effects of endocytic inhibitors on Oregon Green–labeled SBFn endocytosis in Caco-2 Cells

A: Caco-2 cells grown in transwell inserts were incubated for 0 to 30 min at 37°C with 5 nmol/L SBFn labeled with Oregon Green 488, and a gallery of confocal fluorescence microscopy optical slices were obtained and integrated into a Z-axis projection. An initial apical distribution evolved with time to a distribution in both the apical and basal domains. B: Cells were pre-incubated for 15 min with no additions, with filipin, or under hypertonic or acid conditions as described in the Material and Methods. Ten μmol/L Oregon Green–labeled SBFn was added and the incubation was continued for 60 min at 37°C. C: Cells were pre-incubated for 15 min under control, filipin, hypertonic or acid conditions. Five nmol/L ^{131}I-labeled SBFn was added and the incubation was continued for 60 min at 37°C. The difference in intensity of contoro fluorescence in panels A and B reflect the different incubation times of 0-30 and 60 min, respectively. Data are presented as the mean, and the error bars show the SD for three independent experiments. *, $P < 0.05$, and ***, $P < 0.001$ in reference to Control.

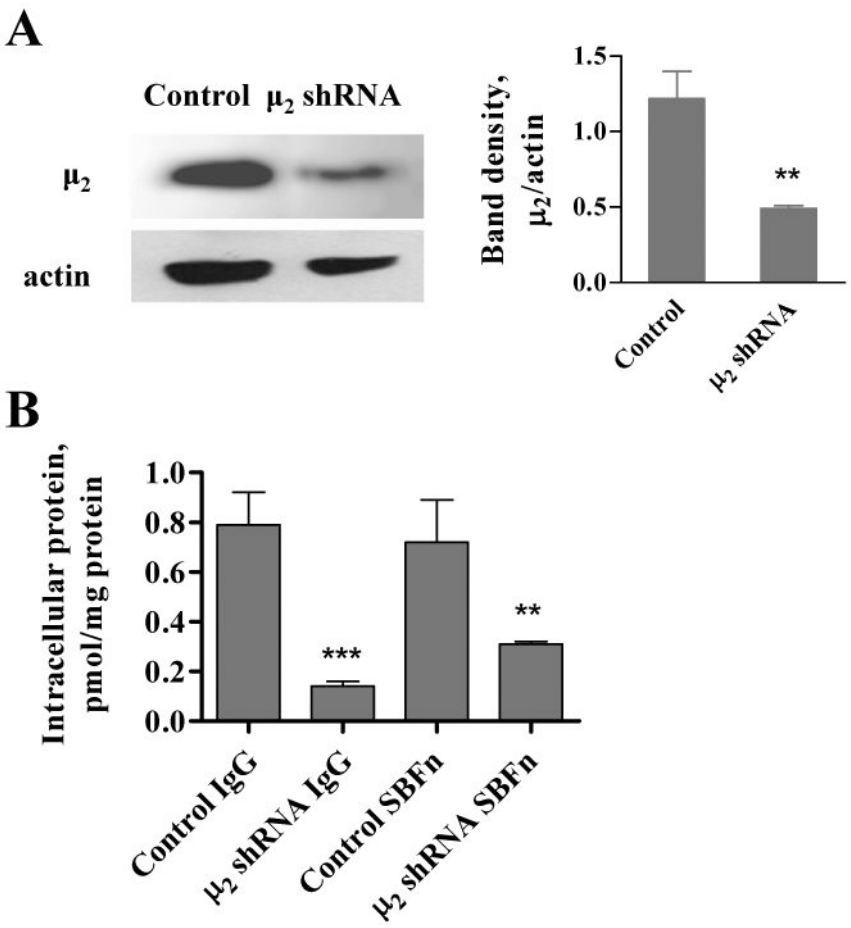

Figure 6. Inhibition of SBFn endocytosis by μ_2 siRNA

A: cells were nucleofected with pSUPER or pSuper-μ_2-shRNA plasmids and 3 days later tested for μ_2 expression by Western blot analysis. Left graph shows mean ± SEM of three independent experiments, (**, P = 0.0022) compared to control. B: ^{131}I-SBFn internalization by cells nucleofected with pSUPER (Control) or pSuper-μ_2-shRNA plasmids. Cells were nucleofected and 3 days later tested for ^{131}I-SBFn (10 nmol/L) or ^{131}I-IgG (15 nmol/L) internalization for 60 min at 37°C. Shown is mean ± SEM of one of three independent experiments, with conditions tested in triplicates. **, P < 0.01 compared to control; ***, P < 0.001 compared to control.